BIOCHEMISTRY
including biophysical chemistry & molecular biology

ARTICLE

pubs.acs.org/biochemistry

A Four-Enzyme Pathway for 3,5-Dihydroxy-4-methylanthranilic Acid Formation and Incorporation into the Antitumor Antibiotic Sibiromycin

Tobias W. Giessen, Femke I. Kraas, and Mohamed A. Marahiel*

Department of Chemistry/Biochemistry, Philipps-University Marburg, Hans-Meerwein-Strasse, D-35032 Marburg, Germany

Supporting Information

ABSTRACT: The antitumor antibiotic sibiromycin belongs to the class of pyrrolo[1,4]benzodiazepines (PBDs) that are produced by a variety of actinomycetes. PBDs are sequence-specific DNA-alkylating agents and possess significant antitumor properties. Among them, sibiromycin, one of two identified glycosylated PBDs, displays the highest DNA binding affinity and the most potent antitumor activity. In this study, we report the elucidation of the precise reaction sequence leading to the formation and activation of the 3,5-dihydroxy-4-methylanthranilic acid building block found in sibiromycin, starting from the known metabolite 3-hydroxykynurenine (3HK). The investigated pathway consists of four enzymes, which were biochemically characterized in vitro. Starting from 3HK, the SAM-dependent methyltransferase SibL converts the substrate to its 4-methyl derivative, followed by hydrolysis through the action of the PLP-dependent kynureninase SibQ, leading to 3-hydroxy-4-methylanthranilic acid (3H4MAA) formation. Subsequently the NRPS didomain SibE activates 3H4MAA and tethers it to its thiolation domain, where it is hydroxylated at the C5 position by the FAD/NADH-dependent hydroxylase SibG yielding the fully substituted anthranilate moiety found in sibiromycin. These insights about sibiromycin biosynthesis and the substrate specificities of the biosynthetic enzymes involved may guide future attempts to engineer the PBD biosynthetic machinery and help in the production of PBD derivatives.

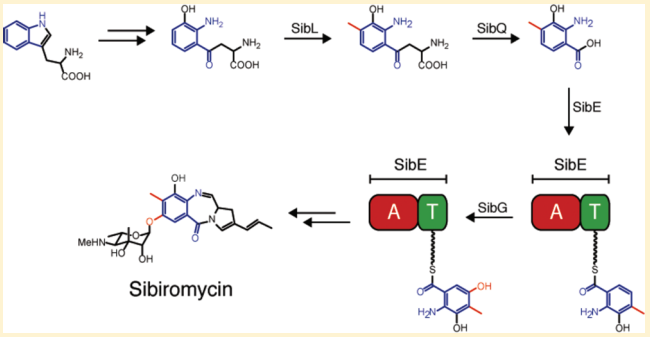

Sibiromycin is an antitumor antibiotic belonging to the class of naturally produced pyrrolo[1,4]benzodiazepines (PBDs).[1] This group of natural products shares a common pyrrolo[1,4]benzodiazepine ring system consisting of fused six-, seven-, and five-membered rings (Figure 1A),[2] where the differing substitution patterns of the anthranilate and pyrrole moieties and the degree and position of unsaturation in the C-ring greatly influence the biological activities.[3] They are sequence-specific DNA-alkylating agents showing significant antitumor properties, which makes them an interesting research topic.[4]

Their biological mode of action consists of establishing a covalent linkage between C11 of the PBD and the exocyclic N2 of a guanine base in double-stranded B-DNA.[5] Because of the right-handed twist of their ring system, resulting from the *S*-configuration of C11a, PBDs fit nicely into the minor groove, causing very little distortion of the overall DNA structure.[5] This makes it more difficult for the DNA repair machinery to recognize and fix this DNA modification compared to DNA adducts resulting from other alkylating agents, which significantly contributes to the potency of PBDs.[6] Sibiromycin, produced by *Streptosporangium sibiricum*, has the highest DNA binding affinity (ΔT_m = 16.3 °C) and cytotoxicity of all known PBDs, including synthetically produced PBDs, with IC_{50} values varying from 4 to 1.7 pM in leukemia, plasmacytoma, and ovarian cancer cell lines.[7] Despite these promising properties, further testing of sibiromycin is precluded because of a dose-dependent cardiotoxicity observed in clinical trials.[8,9] Extensive structure−activity relationship studies established the C9 hydroxyl group in anthramycin, and by analogy in sibiromycin, to be the cause of these cardiotoxic properties.[3,10−12] These studies also showed that O-glycosylation at C7 significantly enhances DNA binding affinity, which is in agreement with sibiromycin possessing the highest potency of all PBDs, being one of only two known glycosylated members of this class, the other being sibanomicin.[13] The promising potencies of PBDs sparked many attempts to synthesize naturally occurring PBDs and synthetic derivatives thereof. While many structurally less complex PBD analogues could be produced synthetically, the routes to more complex natural PBDs were found to be laborious and inefficient in terms of yield.[2] In addition, the synthesis of the glycosylated sibiromycin has not yet been accomplished because of problems related to the synthesis of the corresponding sibirosamine sugar moiety and subsequent aglycon coupling.[2,14−17]

Information concerning the biosynthesis of PBDs is mainly restricted to the anthramycin, tomaymycin, and sibiromycin systems, which have been analyzed to some extent by precursor

Received: April 21, 2011
Revised: May 25, 2011
Published: May 25, 2011

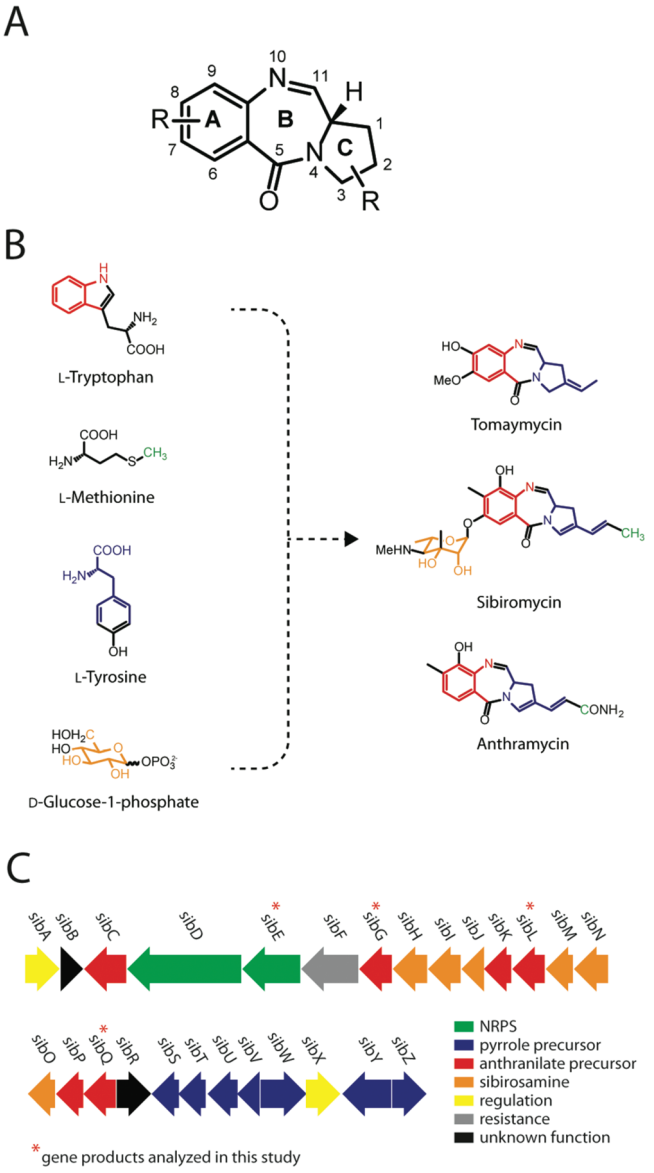

Figure 1. Structure and biosynthesis of PBDs. (A) Pyrrolo[1,4]benzodiazepine ring system highlighting the numbering and designation of the fused rings. (B) Common metabolic precursors and chemical structures of the PBDs tomaymycin, sibiromycin, and anthramycin. (C) Genetic organization of the sibiromycin gene cluster. Panels A and B were partly adapted from ref 23.

feeding experiments and gene deletion studies.[18,19] Those investigations established a close relationship among the three biosynthetic systems, showing that they share common biosynthetic precursors (Figure 1B). The anthranilate moiety is derived from L-tryptophan, the pyrrole moiety from L-tyrosine, the terminal methyl group in the C-ring side chain of sibiromycin from L-methionine, and the sibirosamine sugar moiety from D-glucose 6-phosphate.[18,19] Resistance to PBDs in the producer strains is thought to arise from changes in cell permeability with regard to the antibiotics and to be regulated by their biosynthesis.[20] The gene clusters for anthramycin,[21] tomaymycin,[22] and sibiromycin[23] have recently been identified and functionally annotated through the use of homology analysis, gene inactivation, chemical complementation, and a comparative analysis of the three above-mentioned clusters and the gene cluster of the related lincosamide antibiotic lincomycin (Figure 1C).[24,25] Using those insights, it was possible to postulate a putative biosynthetic route for sibiromycin assembly, in which the anthranilate and dihydropyrrole moieties are synthesized before the NRPS-dependent formation of the diazepine ring system (Figure 2).[23,26] The anthranilate and dihydropyrrole building blocks are activated by the adenylation domains (A-domains) and subsequently tethered to the thiolation domains (T-domains) of NRPS modules SibE and SibD, respectively. After condensation catalyzed by the N-terminal condensation domain (C-domain) of SibD, the dipeptide is released from the assembly line by a two-electron reduction catalyzed by SibD's C-terminal reductase domain (R-domain). After autocatalytic ring closure and formation of the pyrrolo[1,4]benzodiazepine ring system, the sibirosamine moiety is installed on the C7 hydroxyl group of the aglycon by the putative glycosyltransferase SibH, resulting in the formation of the mature natural product. The suggested biosynthesis of the dihydropyrrole moiety starts with the formation of a five-membered ring by a tyrosine hydroxylase (SibU) and an L-DOPA 2,3-dioxygenase (SibV), followed by the successive action of five further enzymes, which install the propenyl side chain and adjust the oxidation level of the five-membered heterocycle.[23,26] With regard to the 3,5-dihydroxy-4-methylanthranilic acid (3,5DH4MAA) moiety found in sibiromycin, it was proposed that starting from L-tryptophan the intermediate 3-hydroxykynurenine is formed via a route analogous to the kynurenine pathway. Furthermore, it could be deduced that all substituents located on the anthranilate moiety are installed before diazepine ring formation, but the precise sequence of reactions leading to the observed substitution pattern remained speculative.[23,26] Similar anthranilate-based building blocks derived from L-tryptophan include 3-hydroxy-4-methylanthranilic acid (3H4MAA), found in several secondary metabolites, including the actinomycins.[21,27] Another related compound is the more widespread 3-hydroxyanthranilic acid (3HAA), which is present in fungi, yeasts, higher eukaryotes, and a limited number of bacteria, excluding actinomycetes, as an intermediate of NAD^+ biosynthesis or L-tryptophan catabolism.[28,29] Nevertheless, previous studies were able to establish a link between 3HAA and 3H4MAA in an actinomycete by the discovery of an enzyme from the actinomycin-producing *Streptomyces antibioticus* that specifically methylates 3HAA at its C4 position, forming 3H4MAA.[30,31]

In this study, we focus on 3,5-dihydroxy-4-methylanthranilic acid formation and its incorporation into sibiromycin. Our approach was to biochemically characterize all proposed enzymes involved in anthranilate formation starting from 3-hydroxykynurenine. For this reason, the SAM-dependent methyltransferase SibL, the PLP-dependent kynureninase SibQ, the FAD/NADH-dependent hydroxylase SibG, and the NRPS didomain SibE, as well as the excised thiolation domain SibE-PCP, were cloned and recombinantly expressed in *Escherichia coli*. Through biochemical in vitro characterization of those enzymes, we were able to establish the precise sequence of reactions leading to the formation and activation of the fully substituted anthranilate moiety found in sibiromycin. Improving our understanding of sibiromycin biosynthesis and elucidating the specificities of the processing enzymes may guide future attempts to engineer the PBD biosynthetic machinery and pave the way to the biocombinatorial synthesis of (glycosylated) PBD derivatives.

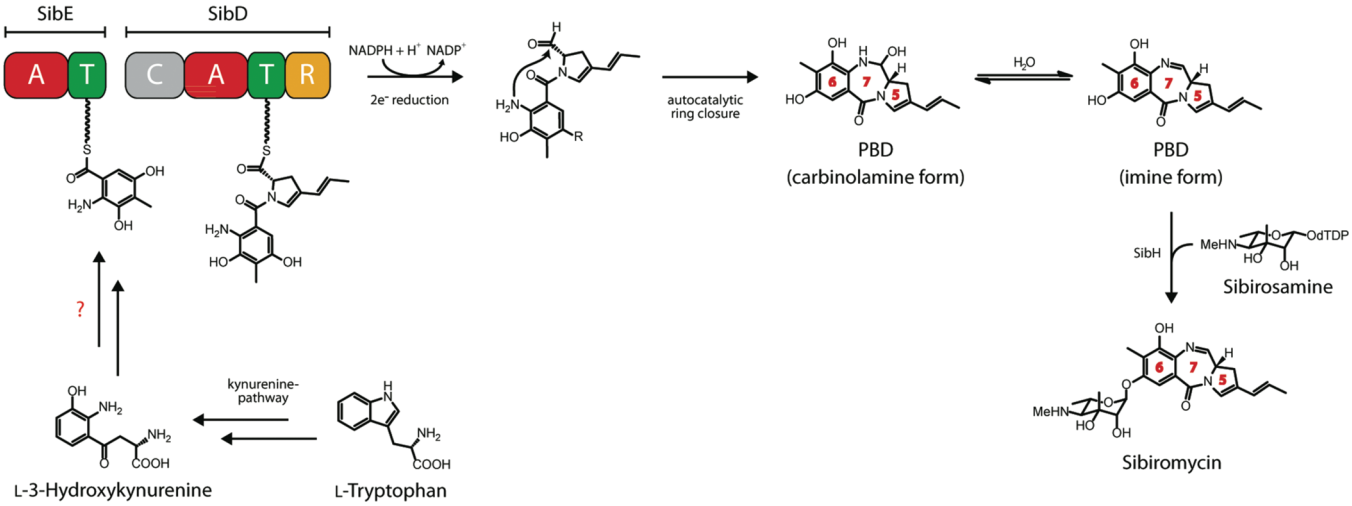

Figure 2. Proposed biosynthetic pathway leading to the anthranilate building block and assembly of the PBD ring system of sibiromycin by NRPS modules SibE and SibD with subsequent transfer of the sibirosamine sugar moiety onto the C7 hydroxyl group of the sibiromycin aglycon.

MATERIALS AND METHODS

Bacterial Strains, Materials, and Instruments. *S. sibiricum* DSM 44093 was obtained from DSMZ, cultivated in liquid ISP4 or GYM medium, and maintained on ISP4 agar plates. *E. coli* TOP10 cells purchased from Invitrogen were used for cloning procedures. *E. coli* BL21(DE3) or *E. coli* Rosetta(DE3) cells (Novagen) transformed with pET-derived vectors were used for overexpression of proteins in LB medium supplemented with kanamycin (50 μg/mL). All chemicals, including oligonucleotide primers and L-amino acid oxidase (*Crotalus atrox*), were purchased from Sigma-Aldrich unless stated otherwise. Phusion High-Fidelity DNA Polymerase (New England Biolabs) was used for polymerase chain reaction (PCR) amplification. DNA sequencing was performed by GATC Biotech. Nickel-nitrilotriacetic acid agarose (Ni-NTA) superflow was purchased from Qiagen. Protein samples were concentrated using Amicon Ultra Filters (Millipore). DNA and protein concentrations were determined with a Nanodrop ND-1000 spectrophotometer (PEQLab) and in the case of SibE-PCP with the Bradford Protein Assay Kit (Bio-Rad). [^{32}P]PP$_i$ was purchased from PerkinElmer.

Preparative HPLC purification was performed on a 1100 Series LC system (Agilent) equipped with a C18 column [Macherey and Nagel, Nucleodur C-18 ec, 250 mm × 21 mm, particle size of 5 μm, pore size of 110 Å, and flow rate of 18 mL/min, with solvent A being 0.1% (v/v) TFA with ddH_2O and solvent B being 0.1% (v/v) TFA with acetonitrile] using gradient elution (0 to 95% B over 30 min). HPLC-MS analysis of reaction mixtures was conducted with an ESI-Quad 1100(A) Series MSD LC-MS system (Agilent). HPLC-MS analysis of proteins was achieved on a qTOF-MS QStar Pulsar i instrument (Applied Biosystems) coupled to an HP 1100 HPLC system (Agilent) equipped with a ProSwift RP-4H column [Dionex, 50 mm × 1 mm, pore diameter of 10^4 Å, and flow rate of 0.2 mL/min, with solvent A being 0.45% (v/v) formic acid with ddH_2O and solvent B being 0.45% (v/v) formic acid with acetonitrile] using gradient elution (5 to 95% B over 8 min). Protein mass reconstruction was assessed using Analyst QS version 1.1 (Applied Biosciences). Nuclear magnetic resonance (NMR) spectra were recorded on a Bruker Avance 300 instrument.

Kinetic parameters were determined by using experimentally obtained starting velocities and the Enzyme Kinetic Module for Sigma Plot 8.0 (SPSS).

Cloning of SibE, SibE-PCP, SibG, SibL, and SibQ. The genes encoding SibE, SibE-PCP, SibG, SibL, and SibQ were amplified by PCR from genomic DNA extracted from *S. sibiricum* using the Phusion High-Fidelity DNA Polymerase with GC buffer according to the manufacturer's protocol. The *sibE* gene was amplified using oligonucleotides 5′-AAA AAA CCA TGG CTT CCG CCC TTC CCT CTC TCC GAG-3′ (NcoI) and 5′-AAA AAA CTC GAG TGC AGG CAC CTC CCG GTG GC-3′ (XhoI). The amplification of *sibE-PCP* was conducted using the primer combination of 5′-AAA AAA CAT ATG GTC CTG GTC GAG CCG GAC GG-3′ (NdeI) and 5′-AAA AAA CTC GAG TGC AGG CAC CTC CCG GTG GC-3′ (XhoI). The gene encoding SibG was amplified using 5′-AAA AAA CAT ATG AGG ATC CTG GTC AAC GGC GGG-3′ (NdeI) as the forward primer and 5′-AAA AAA AAG CTT CCC GCG TAC GGG TAC CGC TC-3′ (HindIII) as the reverse primer. The *sibL* gene was amplified using the primer pair of 5′-AAA AAA CCA TGG CTA GCT CCG AAC TGT CCG CCC TCG-3′ (NcoI) and 5′-AAA AAA GCG GCC GCT CGC GGA CGG CTC CCC GAC A-3′ (NotI). The amplification of *sibQ* was achieved using the primer combination of 5′-AAA AAA CCA TGG CTG AAT CGA CAC GCG GAT GGG CCG-3′ (NcoI) and 5′-AAA AAA CTC GAG CCG CAG CAC CTC CCG CAA GTG-3′ (XhoI). In the case of *sibE-PCP* and *sibG*, the purified and digested PCR products were ligated into the pET41a expression vector and the constructs confirmed by DNA sequencing. For *sibE*, *sibL*, and *sibQ* the purified and digested PCR products were ligated into expression vector pET28a and the sequences confirmed by DNA sequencing.

Production of Recombinant Proteins. The resulting expression constructs of *sibE*, *sibE-PCP*, *sibL*, and *sibQ* were used to transform *E. coli* BL21(DE3) cells. Because of the presence of a rare arginine codon (AGG) following the starting methionine, the expression construct of *sibG* was used to transform *E. coli* Rosetta(DE3) cells. Expression and purification of all five enzymes followed the same general protocol that is detailed here. The transformed cells were grown at 37 °C to an OD_{600}

of 0.3 and subsequently at 25 °C to an OD_{600} of 0.6. The cultures were induced using isopropyl β-D-thiogalactopyranoside (IPTG, final concentration of 0.1 mM) and grown for an additional 18 h at 18 °C. The cells were harvested by centrifugation (7000 rpm for 20 min at 4 °C), resuspended in buffer A [50 mM HEPES, 100 mM NaCl, and 20 mM imidazole (pH 8.0)], and lysed with a French press (SLM Aminco, Thermo French press). Cell debris was removed by centrifugation (17000 rpm for 40 min at 4 °C), and Ni-NTA affinity chromatography was performed using an Äkta Prime system (GE Healthcare Life Sciences). The Ni-NTA column was equilibrated with buffer A, and after the sample had been applied, bound protein was eluted by employing gradient elution with an increasing imidazole concentration [2 to 95% B over 30 min; buffer B contained 50 mM HEPES, 100 mM NaCl, and 200 mM imidazole (pH 8.0)]. Designated protein fractions were identified by sodium dodecyl sulfate−polyacrylamide gel electrophoresis (SDS−PAGE), combined, concentrated, and subjected to buffer exchange [25 mM HEPES and 50 mM NaCl (pH 7.0)] using a HiPrep Desalting Column (GE Healthcare Life Sciences). Obtained proteins were flash-frozen in liquid nitrogen and stored at −80 °C until further use.

Preparation of 3-Hydroxy-4-methylanthranilic Acid. Reduction of 3-hydroxy-4-methyl-2-nitrobenzoic acid to its 2-amino derivative (3-hydroxy-4-methyl-2-anthranilic acid) was conducted according to a procedure developed by Brockman and Muxfeldt.[32] The purification of the product was achieved by preparative HPLC. Lyophilization of the product-containing fractions (t_R = 13.0−14.5 min) yielded 3-hydroxy-4-methylanthranilic acid as a white solid (140 mg, 56%): ^{1}H NMR (300 MHz, C_2D_3N) δ 7.33 (d, J = 8.3 Hz, 1H), 6.45 (d, J = 8.3 Hz, 1H), 2.18 (s, 3H); HR-ESI-MS $[M + H]^+$ m/z 168.0656, theoretical mass m/z 168.0655.

Preparation of 3,5-Dihydroxy-4-methylanthranilic Acid. To a solution of 3,5-dihydroxy-4-methylbenzoic acid (100 mg, 564 μmol) in ethyl acetate (5 mL) cooled to 0 °C using an ice bath was added 65% aqueous nitric acid (19.6 μL, 282 μmol).[33] The reaction mixture was stirred at 0 °C for 15 min, subsequently flash-frozen in liquid nitrogen, and subjected to lyophilization. The resulting yellow powder was dissolved in 5% (v/v) aqueous acetonitrile and purified by preparative HPLC. The product-containing fractions (t_R = 9.5−10.5 min) were freeze-dried, and the resulting yellow powder (11 mg, 11%) of 3,5-dihydroxy-4-methyl-2-nitrobenzoic acid was directly converted to the 2-amino derivative as described previously.[32] Preparative HPLC purification and subsequent lyophilization yielded 3,5-dihydroxy-4-methylanthranilic acid (6 mg, 55%) as a white solid: ^{1}H NMR (300 MHz, C_2D_3N) δ 6.94 (s, 1H), 2.21 (s, 3H); HR-ESI-MS $[M + H]^+$ m/z 184.0604, theoretical mass m/z 184.0604.

Preparation of 3H4MAA-CoA. 3-Hydroxy-4-methylanthranilic acid (3.12 mg, 18.6 μmol), CoA trilithium salt dihydrate (MP Biomedicals; 46.5 mg, 55.8 μmol), and PyBOP (Novobiochem; 49.6 mg, 93.1 μmol) were dissolved in 1.5 mL of a THF/ddH_2O mixture (1:1, v/v). DIPEA (16.2 μL, 93.1 μmol) was then added, and the reaction mixture was stirred at 25 °C for 2 h. After lyophilization and resuspension in 5% aqueous acetonitrile, preparative HPLC was performed. The product-containing fractions (t_R = 18.0−20.5 min) were combined, lyophilized, and yielded 3H4MAA-CoA as a white solid (5.12 mg, 29%): HR-ESI-MS $[M + H]^+$ m/z 917.1702, theoretical mass m/z 917.1702.

Preparation of 3HAA-CoA. 3-Hydroxyanthranilic acid (6.11 mg, 40 μmol), CoA trilithium salt dihydrate (MP Biomedicals; 50.5 mg, 60 μmol), and PyBOP (Novobiochem; 32.2 mg, 60 μmol) were dissolved in 2.0 mL of a THF/ddH_2O mixture (1:1, v/v). DIPEA (69.5 μL, 400 μmol) was then added, and the reaction mixture was stirred at 25 °C for 2 h. After lyophilization and resuspension in 10% aqueous acetonitrile, preparative HPLC was performed. The product-containing fractions (t_R = 15.0−17.0 min) were combined, lyophilized, and yielded 3HAA-CoA as a white solid (10.6 mg, 25%): HR-ESI-MS $[M + H]^+$ m/z 903.1542, theoretical mass m/z 903.1545.

Separation and Stereochemical Analysis of D-/L-3-Hydroxykynurenine. Separation of racemic 3-hydroxykynurenine into its enantiomers was achieved by HPLC using a chiral semipreparative ligand exchange column based on D-penicillamine [Phenomenex, Chirex3126, 250 mm × 4.6 mm, particle size of 5 μm, pore size of 110 Å, and flow rate of 1 mL/min, with solvent A being 2 mM $CuSO_4$ in a ddH_2O/2-propanol mixture (95:5, v/v) and solvent B being 2-propanol] and applying isocratic conditions (5% B). The separated product peaks (t_R = 14.2 and 17.8 min) were collected, and the stereochemistry of the corresponding enantiomers was determined by using L-amino acid oxidase according to the manufacturer's protocol. The assays were analyzed by HPLC-MS [Macherey and Nagel, Nucleodur C18 ec, 125 mm × 4.6 mm, particle size of 3 μm, pore size of 110 Å, and flow rate of 0.3 mL/min, with solvent A being 0.1% (v/v) TFA with ddH_2O and solvent B being 0.1% (v/v) TFA with acetonitrile] using gradient elution (0 to 95% B over 23 min). The first peak (t_R = 14.2 min) was identified as corresponding to L-3-hydroxykynurenine and the second peak (t_R = 17.8 min) to D-3-hydroxykynurenine (Figure S1 of the Supporting Information).

General Methylation Assay. The recombinant methyltransferase SibL (20 μM) was incubated with the cosubstrate *S*-adenosyl-L-methionine (1 mM) and the substrate of interest (500 μM) in 50 μL of 25 mM HEPES and 50 mM NaCl (pH 7.0) at 30 °C for 2 h. The reactions were stopped by addition of TFA [final concentration of 10% (v/v)] and analyzed by HPLC-MS [Macherey and Nagel, Nucleodur C18 ec, 125 mm × 4.6 mm, particle size of 3 μm, pore size of 110 Å, and flow rate of 0.3 mL/min, with solvent A being 0.1% (v/v) TFA with ddH_2O and solvent B being 0.1% (v/v) TFA with acetonitrile] by applying a linear gradient from 0 to 95% B over 23 min. Control reactions were conducted by excluding either SibL or *S*-adenosyl-L-methionine.

When using a SibE-tethered substrate, the didomain SibE (30 μM) was artificially loaded with 3HAA-CoA (300 μM) by using the promiscuous phosphopantetheinyl transferase Sfp (3 μM).[34,35] After the loading reaction had reached completion, SibL (10 μM) and the cosubstrate *S*-adenosyl-L-methionine (500 μM) were added and the reaction mixture was incubated at 30 °C for 2 h. The reaction was stopped by addition of formic acid [final concentration of 10% (v/v)] and analyzed by HPLC-MS.

Exclusion of Racemization during the SibL Methylation Assay. To exclude racemization of 3-hydroxykynurenine as the reason for the apparent promiscuity of SibL with regard to the stereochemistry of its substrate, methylation assays using D- and L-3-hydroxykynurenine were performed, and they were subsequently used as substrates in L-amino acid oxidase assays (vide supra). The analysis of reaction mixtures was conducted via HPLC-MS. Only in assays containing L-3-hydroxykynurenine was the typical oxidation product observed, which confirms that no racemization occurs during SibL methylation assays (Figure S2 of the Supporting Information).

Kinetic Investigations of SibL. The kinetic parameters of SibL were determined with the concentration of *S*-adenosyl-L-methionine maintained at 1 mM and the concentration of D- or

L-3-hydroxykynurenine varied from 0 to 1000 μM. Assays were initiated by the addition of SibL to the reaction mixtures and stopped by addition of TFA [final concentration of 10% (v/v)] after 20 min, which was determined to be an appropriate reaction time for being in the linear conversion range. All reactions were performed in triplicate.

Coupled Methylation−Hydrolytic Cleavage Assay. The methylation assays were conducted as described above. After 2 h, the kynureninase SibQ (14 μM) and the corresponding cofactor pyridoxal 5′-phosphate (14 μM) were added (final assay volume of 150 μL). The reaction mixture was incubated at 30 °C for an additional 30 min and subsequently analyzed via HPLC-MS [Macherey and Nagel, Nucleodur C18 ec, 125 mm × 4.6 mm, particle size of 3 μm, pore size of 110 Å, and flow rate of 0.3 mL/min, with solvent A being 0.1% (v/v) TFA with ddH_2O and solvent B being 0.1% (v/v) TFA with acetonitrile] using gradient elution (0 to 95% B over 23 min).

ATP−[^{32}P]PP$_i$ Exchange Assay. A typical assay contained, in a total volume of 500 μL, 800 μM acid substrate, 1 mM ATP, 10 mM $MgCl_2$, 5 mM $NaPP_i$, and 2 μM SibE. Before the reaction was started by the addition of SibE, 5 μL of a Na[^{32}P]PP$_i$ solution (~2.0×10^7 cpm/mL) was added. The reaction mixure was incubated at 30 °C for 15 min and the reaction subsequently quenched with 750 μL of a charcoal suspension [100 mM $NaPP_i$, 600 mM $HClO_4$, and 1.6% (w/v) charcoal]. After two washing steps using a wash solution (100 mM $NaPP_i$ and 600 mM $HClO_4$), the resuspended charcoal was transferred into 4 mL of scintillation solution (Rotiszint, Carl Roth) and radioactivity measurements were performed using a liquid scintillation analyzer (Packard Tricarb 2100TR). All reactions were performed in triplicate.

Substrate Tethering Assay. The didomain SibE (30 μM) was artificially loaded with CoA (300 μM) by using the promiscuous phosphopantetheinyl transferase Sfp (3 μM).[34,35] The loading reaction mixture additionally contained 3 mM $MgCl_2$, 50 mM NaCl, and 25 mM HEPES (pH 7.0). The reaction mixture was incubated at 30 °C for 15 min, which was determined to be sufficient for complete conversion of the apoprotein to the catalytically active holoprotein. Subsequently, 700 μM ATP and 500 μM acid substrate were added, and the reaction mixture was incubated at 30 °C for an additional 30 min. The assays were stopped by the addition of 5% (v/v) formic acid (final concentration) and subjected to HPLC-MS analysis.

Hydroxylation Assay with SibE-*S*-3H4MAA and SibE-PCP-*S*-3H4MAA. SibE (50 μM) or SibE-PCP (50 μM) was artificially loaded with 3H4MAA-CoA (400 μM) using the promiscuous phosphopantetheinyl transferase Sfp (5 μM) for a reaction analogous to the loading reaction described above. After loading had been completed, SibG (10 μM), FAD (20 μM), and NADH (2 mM) were added to the reaction mixture, which was subsequently incubated at 30 °C for an additional 30 min. The reaction was stopped by the addition of 20% (v/v) formic acid (final concentration) and analyzed via HPLC-MS.

KOH Cleavage of PCP-Bound 3,5DH4MAA. PCP-bound 3,5-dihydroxy-4-methylanthranilic acid was released from the protein by precipitation with 10% TCA followed by hydrolyzation of the base-labile thioester linkage, which was achieved by incubating the precipitate with 100 mM KOH (100 μL) at 70 °C for 15 min. Subsequently, proteins were removed by precipitation using methanol, and the supernatant was analyzed by HPLC-MS using a Hypercarb column [Thermo Electron Corp., 100% carbon, particle size of 5 μm, and pore diameter of 250 Å, with solvent A being aqueous nonafluoropentanoic acid (20 mM) and solvent B being acetonitrile] and gradient elution (0 to 95% B over 25 min).

Kinetic Investigations of SibG. The loading of SibG-PCP with 3H4MAA-CoA and the subsequent hydroxylation of the PCP-bound substrate by SibG were conducted in a manner analogous to that of the reactions described above. The appropriate enzyme concentration of SibG was determined to be 0.25 μM and the reaction time to be 5 min. The kinetic parameters of SibG were determined using SibE-PCP-*S*-3H4MAA as the substrate at a concentration that varied between 0 and 500 μM, while the concentrations of FAD (10 μM) and NADH (1 mM) were held constant. Assays were stopped by the addition of 20% (v/v) formic acid (final concentration) and diluted 1:10 (v/v) with ddH_2O for subsequent HPLC-MS analysis.

RESULTS AND DISCUSSION

Expression and Purification of SibE, SibE-PCP, SibG, SibL, and SibQ. The *sibE*, *sibG*, *sibL*, and *sibQ* genes, as well as the *sibE-PCP* gene fragment from *S. sibiricum*, were amplified and cloned into expression vectors. The corresponding recombinant proteins were overproduced in *E. coli* BL21 or Rosetta as His_6-tagged fusions (SibE, 64.6 kDa; SibG, 39.9 kDa; SibL, 38.9 kDa; SibQ, 42.9 kDa; SibE-PCP, 11.6 kDa) and purified using Ni-NTA affinity chromatography. SDS−PAGE analysis indicated that each protein was isolated in high purity (Figure S7 of the Supporting Information). Protein identity was verified by mass spectrometry, and the following protein yields could be obtained from 1 L of bacterial culture: 7.9 mg of SibE, 9.7 mg of SibG, 4.2 mg of SibL, 1.7 mg of SibQ, and 2.4 mg of SibE-PCP.

SibL Is a Stereochemically Promiscuous SAM-Dependent Methyltransferase. It was previously reported that SibL shares a high degree of sequence homology with ORF19,[36] a proposed SAM-dependent aromatic *C*-methyltransferase located in the anthramycin biosynthetic gene cluster from *Streptomyces refuineus*, and AcmL/AcmI from the actinomycin gene cluster in *Streptomyces chrysomallus*,[37] which were shown to catalyze the transformation of D-3-hydroxykynurenine to the corresponding 4-methyl derivative, as well as the methylation of L-tyrosine, in vitro. Phylogenetic analysis revealed that SibL/ORF19 clusters in a sister clade near AcmL/AcmI, as expected for typical orthologues catalyzing the same reaction. On the basis of those previously reported results, we envisioned that SibL would behave like an aromatic *C*-methyltransferase acting on 3-hydroxykynurenine, which would establish the C8 methylation step in sibiromycin biosynthesis to take place not on the anthranilate, but on the kynurenine scaffold. The assumption that methylation takes place after the C7 hydroxyl group is installed on the aromatic ring of kynurenine is in agreement with the proposed mechanism for aromatic C-methylation by SAM-dependent methyltransferases, which requires a phenolic hydroxyl group in the ortho position with respect to the methylation site, as has been noted for the *C*-methyltransferases CouO and NovO in the biosynthesis of the antibiotics coumermycin and novobiocin, respectively.[38] A phenolate ion is most likely formed and activates the benzene ring in the ortho position, facilitating a nucleophilic attack on the methyl group of *S*-adenosyl-L-methionine. Furthermore, it would be interesting to investigate if SibL shows some degree of stereochemical promiscuity as reported for AcmL/AcmI.[36]

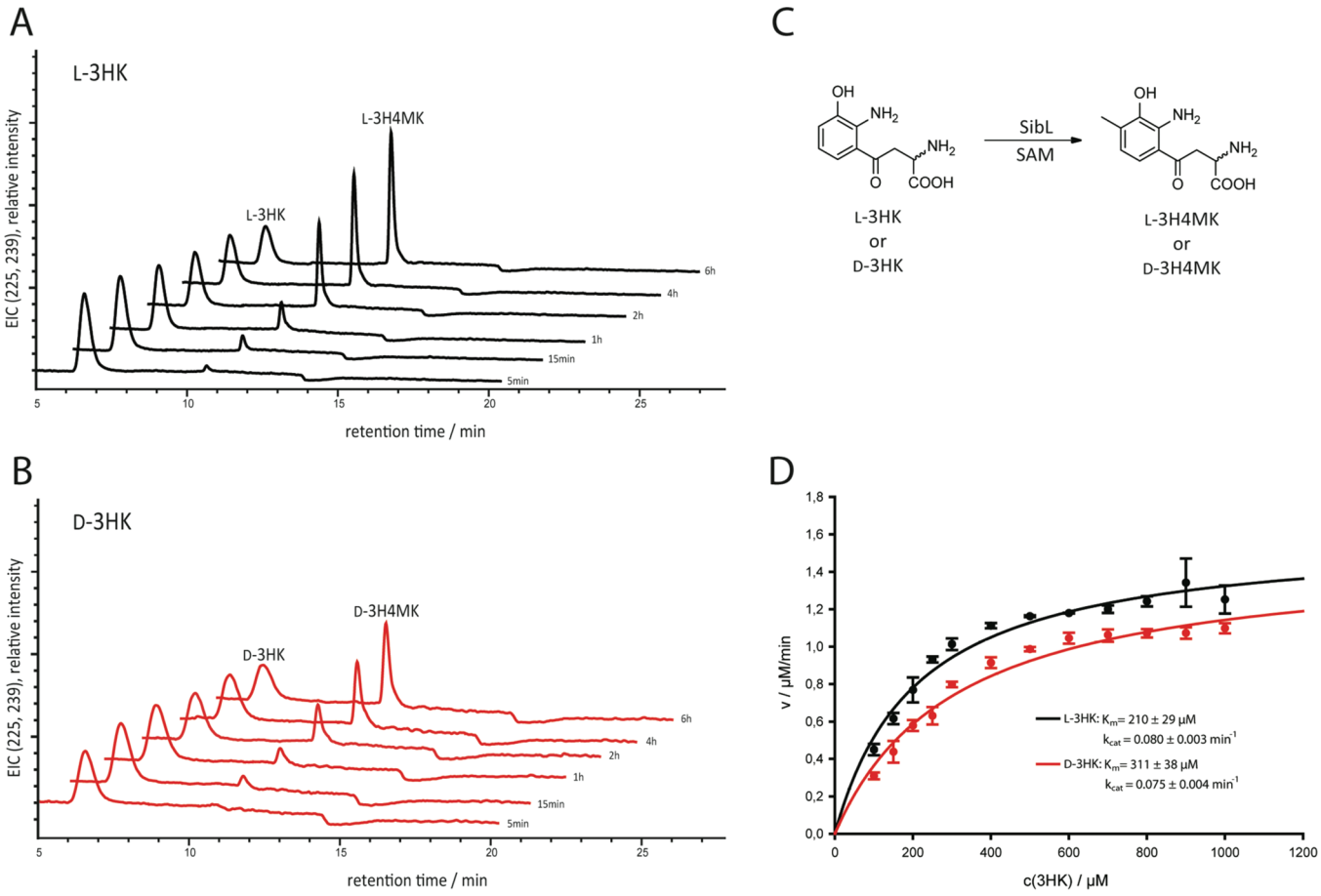

Figure 3. Characterization of SibL as a stereochemically promiscuous SAM-dependent aromatic *C*-methyltransferase. Abbreviations: 3HK, 3-hydroxykynurenine; 3H4MK, 3-hydroxy-4-methylkynurenine. (A) Extracted ion chromatograms (225 Da for $3HK^+$ and 239 Da for $3H4MK^+$) of the time course for the methylation of L-3HK by SibL. The respective reaction times are shown next to the chromatographic traces. (B) Extracted ion chromatograms (225 Da for $3HK^+$ and 239 Da for $3H4MK^+$) of the time course for the methylation of D-3HK by SibL. The respective reaction times are shown next to the chromatographic traces. (C) Chemical transformation catalyzed by SibL. (D) Kinetic characterization of SibL using both L- and D-3HK as substrates, showing the obtained kinetic parameters. Error bars represent standard deviations from three independently performed experiments.

To determine the biosynthetic origin of the C8 methyl group found in the A-ring of sibiromycin, we incubated SibL with commercially available racemic 3-hydroxykynurenine and the corresponding cosubstrate *S*-adenosyl-L-methionine (Figure 3). HPLC-MS analysis revealed the time-dependent formation of a new compound with a mass of 238 Da, corresponding to 3-hydroxy-4-methylkynurenine. This result confirmed our assumption that SibL would act on 3-hydroxykynurenine to generate the 4-methyl derivative thereof, installing the methyl group indeed before anthranilate formation. To further elucidate the substrate specificity, we tested if the methylation of substrates that are structurally similar to 3-hydroxykynurenine could be performed by SibL (Table S1 of the Supporting Information). It was found that in contrast to AcmL/AcmI none of the additionally tested compounds were suitable substrates of SibL, indicating that the longer side chain of 3-hydroxykynurenine, compared to anthranilate or aromatic amino acid substrates, is important for substrate recognition or methylation of the aromatic ring. To exclude the possibility of methylation at a later stage in the biosynthesis, namely at the stage of free or SibE-bound 3HAA, we incubated both substrates with SibL and the appropriate cosubstrate. In both cases, no methylation could be observed (Table S1 of the Supporting Information).

Turning again to the question of stereochemical promiscuity as observed in the AcmL/AcmI orthologues, we set out to test both enantiomeric forms of 3-hydroxykynurenine separately for their potential as methylation substrates of SibL. For that, we developed a HPLC separation strategy employing a chiral stationary phase based on D-penicillamine, followed by identification of the two separated isomers using a promiscuous L-amino acid oxidase (Figure S1 of the Supporting Information). HPLC-MS analysis showed that, indeed, both enantiomers of 3-hydroxykynurenine were accepted as substrates of SibL (Figure 3A,B), extending the sequential homology of AcmL/AcmI and SibL to the functional level by establishing that all three enzymes show a relaxed specificity regarding the stereo configuration of the α-carbon in their substrates. To exclude the possibility of racemization during the assays, which could in principle also account for the observed results, we performed coupled assays, adding sequentially SibL and L-amino acid oxidase. Prompted by the fact that the oxidation product could be detected only in assays employing L-3HK as the substrate, we were able to conclude that no racemization did occur during the methylation assays (Figure S2 of the Supporting Information).

To further characterize SibL, the kinetic parameters for D- and L-3-hydroxykynurenine were determined (Figure 3D). The

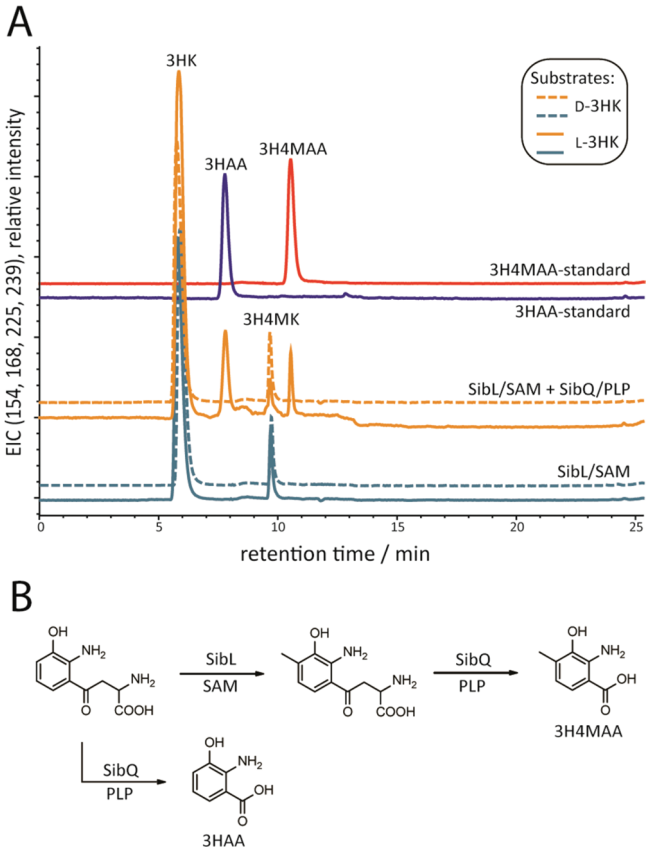

Figure 4. Characterization of SibQ as a PLP-dependent kynureninase. (A) Coupled methylation−hydrolytic cleavage assay (orange). Control reaction without SibQ and PLP (light blue). Standards of 3-hydroxyanthranilic acid (3HAA) and 3-hydroxy-4-methylanthranilic acid (3H4MAA) (dark blue and red, respectively). Dashed LC−MS traces indicate the use of D-stereoisomers as substrates. Abbreviations: 3HK, 3-hydroxykynurenine; 3H4MK, 3-hydroxy-4-methylkynurenine. All traces shown represent extracted ion chromatograms (154 Da for $3HAA^+$, 168 Da for $3H4MAA^+$, 225 Da for $3HK^+$, and 239 Da for $3H4MK^+$). (B) Chemical reactions catalyzed by SibL and SibQ resulting in the formation of 3HAA and 3H4MAA.

lower K_m value found for L-3-hydroxykynurenine ($210 \pm 29\ \mu M$) compared to that of D-3-hydroxykynurenine ($311 \pm 38\ \mu M$) indicates a higher affinity of SibL for the L-enantiomer, pointing toward the possibility that the L-stereoisomer might be the main substrate in vivo (vide infra). The apparent rates for both substrates ($0.080 \pm 0.003\ min^{-1}$ for L-3HK and $0.075 \pm 0.004\ min^{-1}$ for D-3HK) were lower, but in the same range as the rates observed for the related AcmL/AcmI enzymes (k_{cat} for both AcmL and AcmI being $0.11 \pm 0.02\ min^{-1}$).[36] Compared with those of the unrelated aromatic *C*-methyltransferases CouO and NovO, the k_{cat} values of SibL were lower and the K_m values higher (for CouO, $k_{cat} = 2.2 \pm 0.25\ min^{-1}$ and $K_m = 52.0 \pm 4.5\ \mu M$; for NovO, $k_{cat} = 0.5 \pm 0.02\ min^{-1}$ and $K_m = 26.5 \pm 5.5\ \mu M$),[38] indicating an overall greater catalytic efficiency for the CouO/NovO class of *C*-methyltransferases.

The biosynthetic significance of the observed promiscuity of SibL regarding the stereochemistry of its substrate will be more thoroughly discussed in the following section.

PLP-Dependent Cleavage of Kynurenine Derivatives by SibQ. The putative kynureninase SibQ possesses the canonical PLP binding domain characteristic of this class of enzymes,[39] which catalyze cleavage of the $C_\beta-C_\gamma$ bond of kynurenine derivatives based on a mechanism involving the formation of a tautomerized Schiff base employing PLP, attack of an enzyme nucleophile on the C_γ carbonyl, and subsequent hydrolysis of the acyl−enzyme intermediate yielding an anthranilic acid derivative and alanine as the reaction products.[39,40] There are two different types of kynureninases in nature with differing substrate specificities. While the bacterial enzyme involved in L-tryptophan catabolism reacts with L-kynurenine forming anthranilic acid as a reaction product,[41] the eukaryotic kynureninase, also called hydroxykynureninase, involved in NAD^+ biosynthesis, prefers 3-hydroxykynurenine as a substrate leading to 3-hydroxyanthranilic acid formation.[42,43] A way to discriminate between those two types of kynureninases was previously suggested on the basis of functional and structural studies of kynureninase-type enzymes, where the substrate specificity is influenced by a distinctive signature in the substrate-binding pocket of the enzyme.[39] The residues involved are H102 and S332 of the human kynureninase sequence, which are characteristic of hydroxykynureninases, while kynureninases using L-kynurenine as a substrate show W102 and G332 signatures. Recently published work presented an interesting finding regarding a kynureninase enzyme found in the actinomycin system from *St. chrysomallus*, where the enzyme AcmH displayed a specificity signature consisting of W102 (kynureninase-type) and S332 (hydroxykynureninase-type), while being able to convert both kynurenine and 3-hydroxykynurenine to the corresponding anthranilate derivatives with comparable efficiencies.[37] The kynureninase SibQ located in the sibiromycin gene cluster from *S. sibiricum* surprisingly exhibits the specificity signature of a typical L-kynurenine-converting enzyme (W102 and G332), despite the fact that biochemical logic would suggest 3-hydroxy-4-methylkynurenine (3H4MK) as the main substrate based on the observed substrate specificity of the methyltransferase SibL (vide supra).

To investigate the enzymatic capabilities of SibQ in vitro and to test 3H4MK as a substrate, we performed coupled assays, first transforming 3-hydroxykynurenine (3HK) to 3H4MK using SibL, followed by incubation with SibQ and the corresponding cofactor PLP (Figure 4). This was necessary because of the commercial unavailability of 3H4MK. HPLC-MS analysis of the reaction mixture showed that SibQ was able to transform both 3HK and the methylation product 3H4MK to the corresponding anthranilate derivatives indicated by the appearance of two new peaks corresponding to masses of 154 and 168 Da that coeluted with the standards for 3HAA and 3H4MAA, respectively (Figure 4A). Control reactions lacking SibQ and PLP showed no sign of anthranilate formation. Additionally, kynurenine could be used as a substrate by SibQ, forming anthranilic acid (AA) as a reaction product (Table S2 of the Supporting Information). This

Table 1. Specificity-Conferring Amino Acids and Experimentally Determined Substrate Specificities of SibE, ORF21, TomA, and AcmA

A-T didomain	active site residues	substrate	product[a]
SibE	AATNISAALK	3H4MAA[b]	Sib
ORF21	AATNISAALK	3H4MAA (*56*)	Ant
TomA	AAISLSGSIK	?	Tom
AcmA	NMMYVGVLI-	3H4MAA (*55*)	Act

[a] Abbreviations: Sib, sibiromycin; Ant, anthramycin; Tom, tomaymycin; Act, actinomycin. [b] Established in this study.

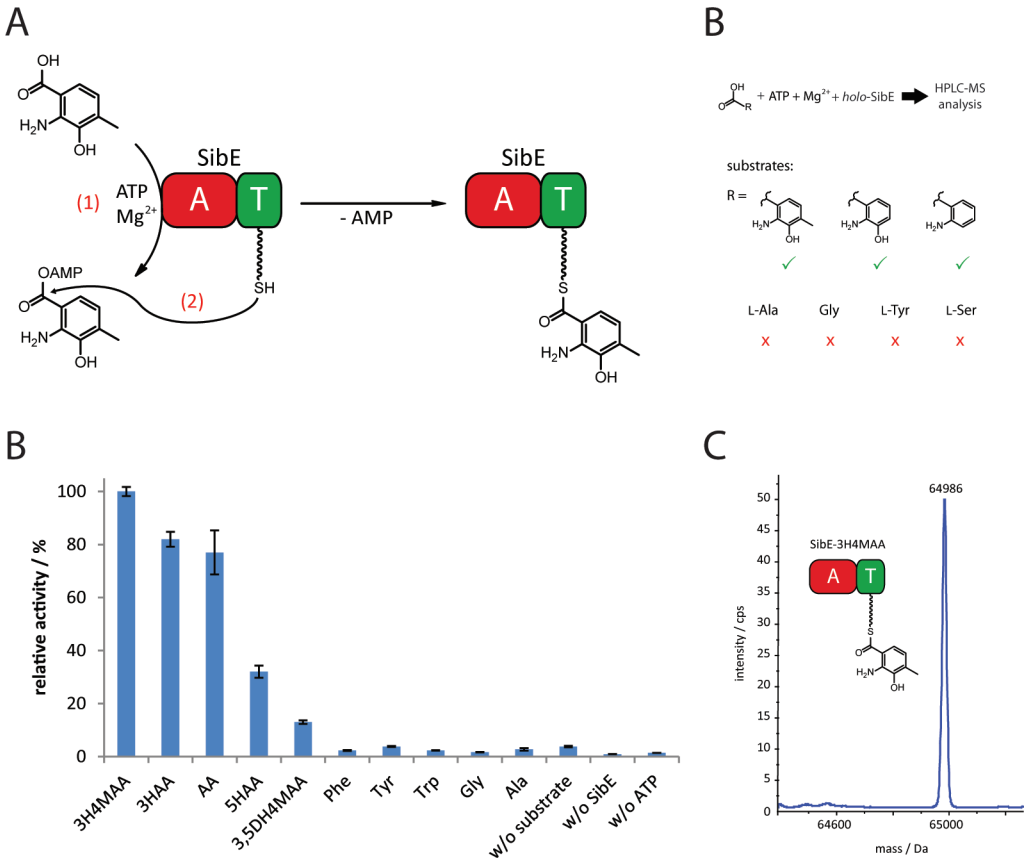

Figure 5. Characterization of SibE substrate specificity. (A) Reaction catalyzed by the A-T didomain SibE. (1) First half of the reaction, in which the acid substrate is activated as an adenylate. (2) Thiolation step by which the activated substrate is covalently tethered to the T-domain. (B) Relative activities obtained from the ATP−[^{32}P]PP$_i$ exchange assay for SibE. Error bars represent standard deviations from three independently performed experiments. (C) Results observed in the substrate tethering assay. The three tested anthranilate derivatives were tethered to SibE (green check mark), whereas no tethering for the tested α-amino acids could be observed (red X). (D) Examplary qTOF-MS data from the 3-hydroxy-4-methylanthranilic acid assay, where the observed mass of 64986 Da corresponds to SibE covalently linked to 3H4MAA. Abbreviations: 3H4MAA, 3-hydroxy-4-methylanthranilic acid; 3HAA, 3-hydroxyanthranilic acid; AA, anthranilic acid; 5HAA, 5-hydroxyanthranilic acid; 3,5DH4MAA, 3,5-dihydroxy-4-methylanthranilic acid.

broad substrate specificity is surprising considering the fact that inhibition of human hydroxykynureninase by L-kynurenine was previously reported.[44] The observed relaxed substrate specificity with regard to the substitution pattern on the anthranilate part of the kynurenine derivative indicates that despite the presence of a specificity signature generally found in L-kynurenine-hydrolyzing enzymes it is necessary to biochemically characterize kynureninases to gain thorough insights into their actual substrate specificities.

Turning now to the stereochemistry of the tested substrates, we were able to show that in all cases only the L-stereoisomer was accepted (Figure 3A and Table S2 of the Supporting Information). This finding is in agreement with previous results that showed no hydrolyzation of D-kynurenine upon incubation with the kynureninase from *Pseudomonas marginalis*[45] and even an inhibitory effect of D-kynurenine on human hydroxykynureninase.[44] The fact that only L-enantiomers of kynurenine derivatives are acceptable substrates of SibQ indicates that the observed stereochemical promiscuity of SibL likely plays no role in vivo and is only an in vitro artifact.

Activation and Tethering of 3H4MAA by the NRPS Didomain SibE. SibE represents a NRPS didomain consisting of an A-domain and a T-domain (also called PCP, peptidyl carrier protein). Both belong to the canonical set of domains found in all functional NRPS modules, where the A-domain is responsible for selection and activation of a substrate by utilizing ATP to form an adenylate with a substrate carboxyl group, while the T-domain functions as the site for subsequent substrate tethering to the NRPS enzyme by which it is sequestered from the cellular pool of soluble metabolites.[46,47] Now the PCP-bound substrate can undergo further modifications catalyzed by tailoring enzymes, followed by condensation with the PCP-bound building block of the downstream module catalyzed by the downstream C-domain.[47,48] Before substrate tethering can occur, the apo-T-domain has to be transformed into the holo form by attachment of a 4′-phosphopantetheine cofactor to a conserved serine residue through a dedicated phosphopantetheinyl transferase.[47] In general, the use of A-T didomains is a strategy for sequestering a fraction of the pool of a proteinogenic amino acid or other metabolite and modifiying it for use in secondary metabolic pathways and for incorporation into natural products.[47,49,50]

The substrate specificity of bacterial A-domains can be predicted by using various web-based resources such as the NRPS predictor,[51] which are based on the so-called "nonribosomal code" consisting of 10 specificity-conferring amino acid residues located between the A-domain's A4 and A5 core motifs.[52−54] Using those online tools, no prediction for the sibiromycin A-T didomain SibE was achieved. The extracted residues for SibE,

dx.doi.org/10.1021/bi2006114 |*Biochemistry* 2011, 50, 5680–5692

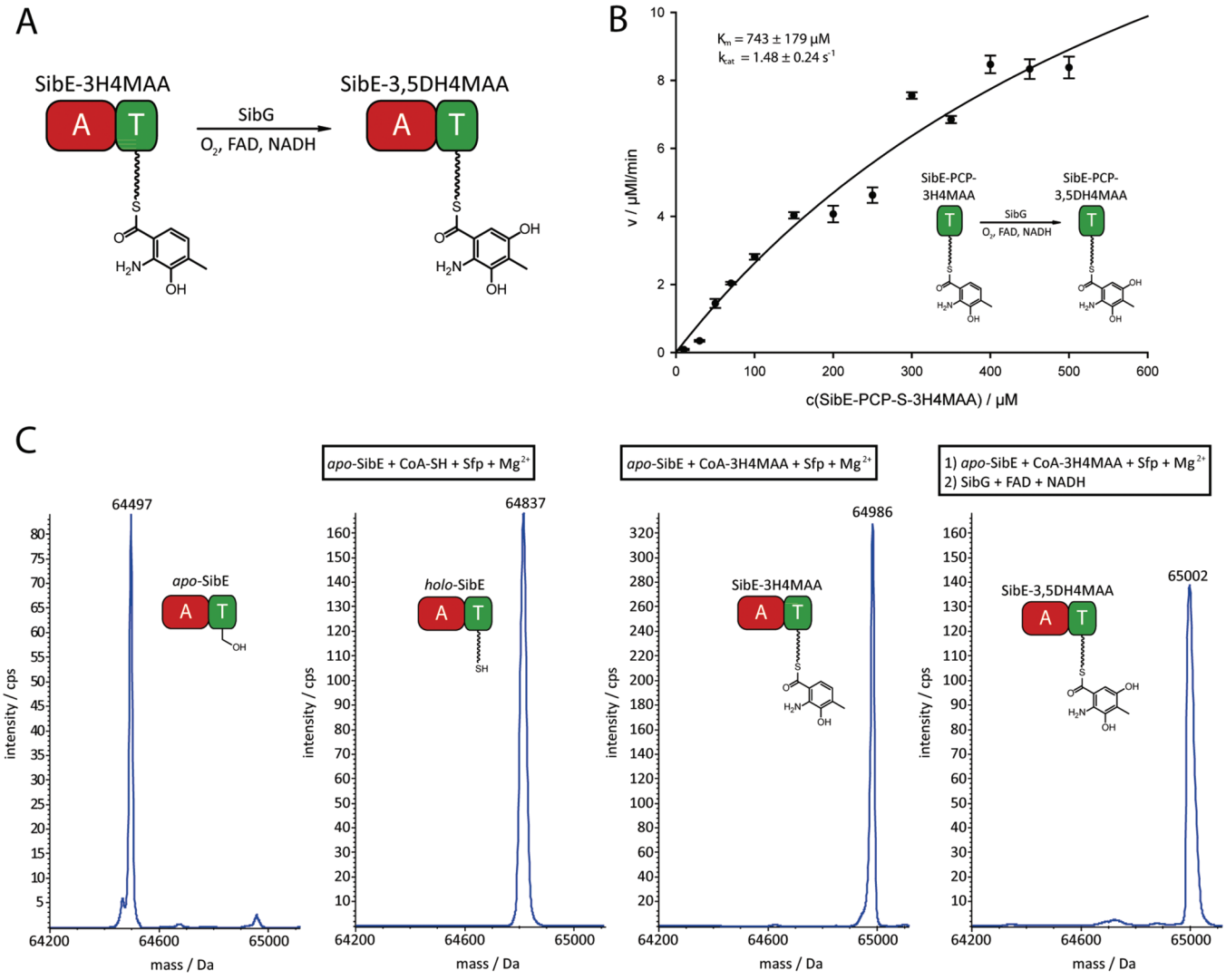

Figure 6. Characterization of SibG as a FAD/NADH-dependent hydroxylase. (A) Hydroxylation of PCP-bound 3H4MAA by SibG, employing the cosubstrates and cofactors NADH, O_2, and FAD. (B) Kinetic characterization of SibG using SibE-PCP-*S*-3H4MAA as the substrate. Error bars represent standard deviations from three independently performed experiments. (C) qTOF-MS data from left to right for apo-SibE (64497 Da), holo-SibE (64837 Da), 3H4MAA-SibE (64986 Da), and 3,5DH4MAA-SibE (65002 Da). The corresponding reactions are shown above the MS data.

and for the homologous A-T didomains in the related anthramycin (ORF21) and tomaymycin (TomA) systems, as well as for the didomain AcmA found in the actinomycin system of *St. chrysomallus* are listed in Table 1. Via analysis of those specificity signatures, it is directly apparent that in all cases the aspartate residue at position 1, which is generally observed in α-amino acid-activating A-domains, is substituted with an uncharged residue. This indicates that the activated substrate may not be an α-amino acid, but as proposed an aryl *β*-amino acid (anthranilic acid derivative). Among the enzymes listed, AcmA and ORF21 were previously biochemically characterized with regard to their substrate specificities.[55,56] Those results showed that 3H4MAA is the main substrate of ORF21's A-domain, while 3HAA was activated to a lesser extent. In the case of AcmA, similar activities for 3H4MAA and 3HAA as well as AA could be observed. Comparison of the active site residues found in SibE and ORF21 shows that all positions are perfectly conserved, strongly suggesting that SibE activates preferentially 3H4MAA as well. To verify this assumption, we tested SibE's function using the classical ATP−[^{32}P]PP$_i$ exchange assay, by which the adenylation half of the two-step reaction catalyzed by an A-T NRPS didomain may be monitored (Figure 5A). The obtained results indicate that, indeed, 3H4MAA is the preferred substrate of SibE. Additionally, side specificities for 3HAA and AA were observed, while all the tested proteinogenic α-amino acids showed only background-level activity (Figure 5B), in agreement with the specificities of the already characterized enzymes ORF21 and AcmA. The fact that 3,5DH4MAA shows a significantly reduced activity in the ATP−[^{32}P]PP$_i$ exchange assay compared to those of the other tested anthranilic acid derivatives indicates that the C7 hydroxyl group found in the aglycon of sibiromycin is installed after activation of 3H4MAA by SibE, which will be discussed in more detail below.

Taking all the results mentioned above into account, we find that it seems that the planar spatial arrangement of the carboxyl and amino groups in anthranilate derivatives is crucial for the activation by the corresponding A-domains. Additionally, in the case of SibE, a more relaxed specificity regarding the substituents at the C3 and C4 positions could be observed, whereas the

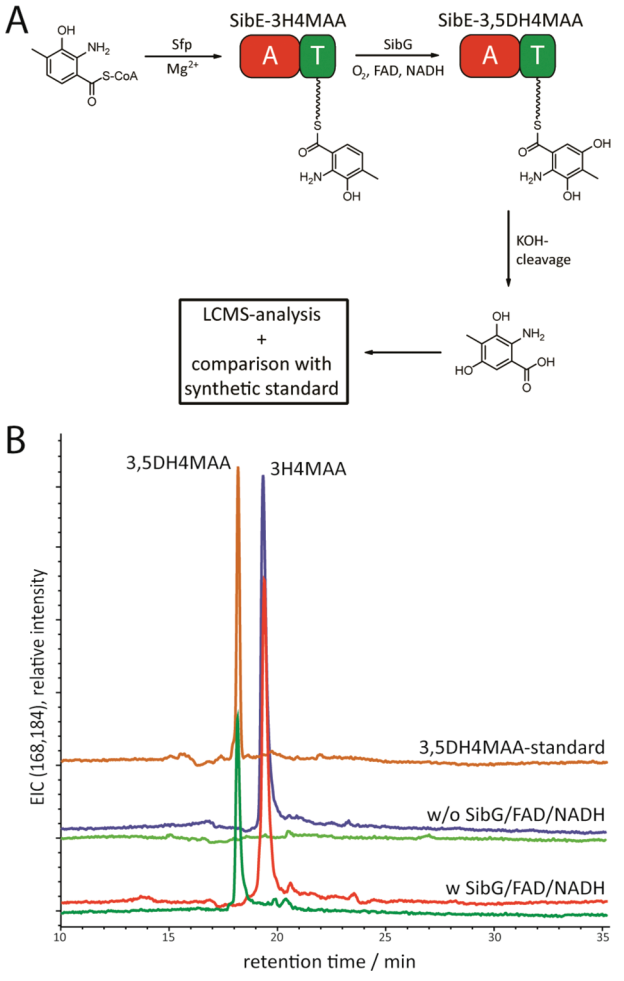

Figure 7. Identification of the SibG reaction product. (A) Outline for the identification of the hydroxylated reaction product of the SibG-catalyzed reaction by KOH cleavage and subsequent HPLC-MS analysis. (B) HPLC-MS traces of the cleaved hydroxylation product and the corresponding standard. All traces shown represent extracted ion chromatograms [168 Da for $3H4MAA^+$ (red and blue) and 184 Da for $3,5DH4MAA^+$ (green and orange)].

presence of a C5 hydroxyl group (5HAA or 3,5DH4MAA) seemed to disturb activation.

Turning to the second step of the A-T didomain-catalyzed reaction, namely the thiolation step, we performed substrate tethering assays by incubating holo-SibE with the corresponding acid substrates and the appropriate cosubstrates (ATP and Mg^{2+}) followed by HPLC-MS analysis (Figure 5C). The findings were in agreement with the activities observed in the ATP−[^{32}P]PP_i exchange assays. Only in the case of anthranilate derivatives could an appropriate mass shift be observed, which indicates that only they were covalently tethered to the holo-SibE didomain (Figure 5C,D).

Hydroxylation of PCP-Bound 3H4MAA by the FAD/NADH-Dependent Hydroxylase SibG. On the basis of mutational studies and complementation experiments, SibG was proposed to be involved in C7 hydroxylation of the anthranilate moiety of sibiromycin, where the installation of the hydroxyl group would take place before diazepine ring formation.[23] In general, two possibilities exist. SibG would either act on the free precursor (3H4MAA) or catalyze the hydroxylation of the PCP-bound anthranilate, a strategy often employed in secondary metabolism to modify monomeric building blocks.[48]

Sequence analysis revealed that SibG possesses the canonical FAD and NADH/NADPH binding sites, while sharing a high degree of sequence homology with salicylyl-CoA 5-hydroxylases, among them SdgC (37% identical) from *Streptomyces* sp. WA46, which was shown to catalyze the C5 hydroxylation of salicylyl-CoA in vitro, resulting in the formation of gentisyl-CoA.[57] These bioinformatic data combined with the insights gained by determination of the SibE substrate specificity suggest that SibG likely hydroxylates PCP-bound 3H4MAA, leading to the formation of the fully substituted anthranilate moiety found in sibiromycin. To test this hypothesis and establish the stage at which hydroxylation occurs, we incubated SibG with FAD and NADH or NADPH as an electron source, as well as with different anthranilic acid derivatives, to experimentally exclude hydroxylation at the stage of the free precursor. Subsequent HPLC-MS analysis showed that, indeed, none of the tested substrates could be hydroxylated by SibG (Table S3 of the Supporting Information). Now we moved on to test if SibG would be able to hydroxylate PCP-bound 3H4MAA, proposed to be the correct substrate when considerations mentioned above are taken into account. Therefore, we artificially loaded the apo didomain SibE using Sfp and 3H4MAA-CoA, followed by incubation with SibG and the appropriate cosubstrates (Figure 6A). HPLC-MS analysis first showed that SibG could indeed hydroxylate PCP-bound 3H4MAA, indicated by a mass shift of 16 Da after incubation with SibG (Figure 6C). Second, it demonstrated that only NADH was accepted as an electron source. To actually prove that PCP-bound 3H4MAA is formed upon incubation with SibG, as indicated by the observed mass shift, we performed a KOH cleavage of the thioester-bound anthranilate and subsequently compared it to a chemically synthesized 3,5DH4MAA standard using HPLC-MS analysis (Figure 7A). The obtained results, showing identical retention times for the standard and the cleaved compound, indeed prove that SibG hydroxylates the C5 position of PCP-bound 3H4MAA (Figure 7B).

To further characterize SibG, we determined the kinetic parameters for 3H4MAA-*S*-SibE-PCP (Figure 6B). Using the excised PCP domain SibE-PCP was necessary, because SibE could not be obtained at concentrations sufficiently high for kinetic characterization. The apparent kinetic parameters (K_m = 743 ± 149 μM; k_{cat} = 88.8 ± 14.4 min^{-1}) indicate that SibG possesses an affinity similar to that of the employed substrate as does the FAD/NADPH-dependent hydroxylase PvdA from *Pseudomonas aeruginosa* for its substrate ornithine, while the possibility that using the excised PCP domain of SibE may lead to a lowering of substrate affinity compared with that of the intact SibE didomain cannot be excluded. In general, modifying enzymes acting on PCP-bound substrates exhibit greater substrate affinities than similar enzymes using free substrates, as exemplified by the non-heme iron oxygenases KtzO from *Kutzneria* sp. (K_m = 121.5 ± 28.1 μM),[58] which acts on PCP-bound glutamic acid, and VioC from *Streptomyces vinaceus* (K_m = 3400 ± 450 μM),[59] which hydroxylates free arginine. Compared with the class of heme-dependent P450 monooxygenases like AziB1 from *Streptomyces sahachiroi* (K_m = 2.4 ± 0.4 μM),[60] which acts on free 5-methylnaphthoic acid, all other mentioned hydroxylases, including SibG, show much greater K_m values, indicating an especially high substrate affinity of heme-dependent hydroxylases. With regard to the turnover rate of SibG, it can be noted that it is greater than the rates of other hydroxylases

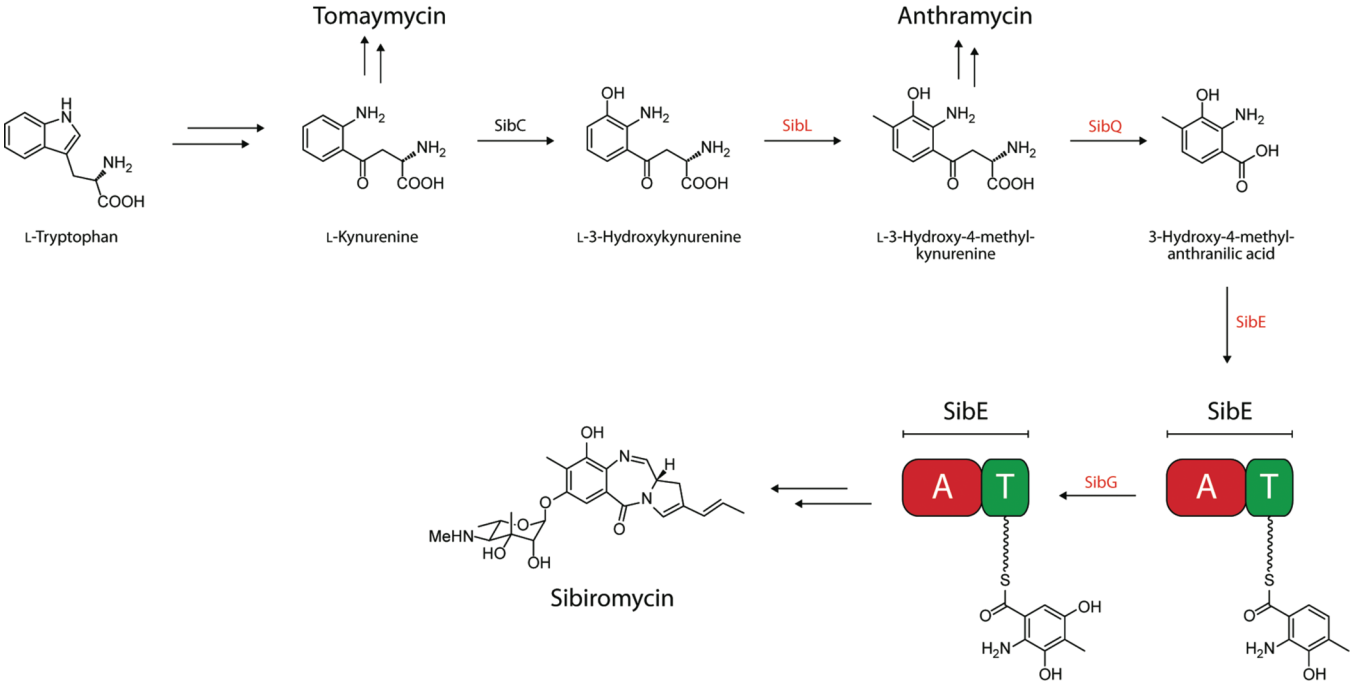

Figure 8. Summary of the investigated enzymatic steps leading to the formation and activation of the 3,5DH4MAA building block in sibiromycin biosynthesis. Enzymes characterized in this study are colored red. The last common precursors in the syntheses of the related PBDs tomaymycin and anthramycin are indicated by additional arrows.

acting on PCP-bound substrates (e.g., k_{cat} = 0.34 ± 0.03 min^{-1} for KtzO),[58] resembling more closely the rates observed for hydroxylases using free substrates (e.g., k_{cat} = 298.8 ± 19.2 min^{-1} for AsnO from *Streptomyces coelicolor*).[61]

CONCLUSIONS

The question we set out to answer concerned the precise order of reaction steps leading to 3,5DH4MAA formation and activation for subsequent incorporation into the sibiromycin molecule. Therefore, we biochemically characterized the four enzymes proposed to be involved in anthranilate formation, starting from the known metabolite 3-hydroxykynurenine. First, we established that SibL is a SAM-dependent aromatic *C*-methyltransferase acting on L- and D-3-hydroxykynurenine, showing that the C8 methyl group found in sibiromycin is installed on the kynurenine and not the anthranilate scaffold. The observed stereochemical promiscuity of SibL was dismissed as an in vitro artifact due to the observed substrate specificities of the downstream enzymes leading to 3,5DH4MAA formation. Turning to SibQ, we were able to show that it belongs to the class of PLP-dependent kynureninases while displaying a relaxed substrate specificity regarding the C3, C4, and C5 substituents of the benzene ring in the kynurenine scaffold. Subsequent investigation of the two half-reactions catalyzed by the NRPS didomain SibE showed a clear preference for anthranilate derivatives, indicating that the corresponding A-domain recognizes only aryl β-amino acids. 3H4MAA could be identified as the preferred substrate, directly suggesting that the C5 hydroxylation of the anthranilate moiety takes place on the PCP-bound intermediate. To verify this hypothesis, we characterized SibG and were able to show that it is a FAD/NADH-dependent hydroxylase indeed acting on PCP-bound 3H4MAA. Those new insights allowed us to establish the precise sequence of reactions leading to the formation of the highly substituted anthranilate moiety found in the antitumor antibiotic sibiromycin, starting with the known metabolite L-3-hydroxykynurenine (Figure 8). Extending our results to the related PBD system of anthramycin, we suggest that the C8 methyl group found in the mature natural product is introduced by the SibL homologue ORF19 using L-3HK as the substrate analogous to the sibiromycin system. Future work on the sibiromycin system will focus on the biochemical characterization of NRPS module SibD, the reductive mechanism employed to release the intermediate from the NRPS assembly line, and the formation of the central seven-membered B-ring found in the mature PBD scaffold of sibiromycin. Additionally, investigations will involve the characterization of putative glycosyltransferase SibH in terms of substrate specificity regarding both the sugar moiety and the aglycon.

To the best of our knowledge, this is the first biochemical characterization of a pathway leading to anthranilate formation and activation in a pyrrolo[1,4]benzodiazepine system. This work may guide engineering attempts of the PBD biosynthetic machinery and function as a starting point for future experiments regarding the biocombinatorial synthesis of (glycosylated) PBD derivatives.

ASSOCIATED CONTENT

Supporting Information. Separation of racemic 3-hydroxykynurenine, substrate specificity of SibL, exclusion of racemization during the SibL methylation assays, substrate specificity of SibQ, qTOF-MS spectra of the SibE tethering assays, UV−vis spectrum of SibG, substrate specificity of SibG (free substrates), ^{1}H NMR spectra of 3H4MAA and 3,5DH4MAA, and SDS−PAGE gel that contained SibE, SibE-PCP, SibG, SibL, and SibQ. This material is available free of charge via the Internet at http://pubs.acs.org.

AUTHOR INFORMATION

Corresponding Author

*Department of Chemistry, Philipps-University Marburg, D-35043 Marburg, Germany. Telephone: +49 (0) 6421 28 25722. Fax: +49 (0) 6421 28 22191. E-mail: marahiel@staff.uni-marburg.de.

Funding Sources

This work has been supported by the Deutsche Forschungsgemeinschaft and the LOEWE Center for Synthetic Microbiology (SYNMIKRO).

ACKNOWLEDGMENT

We thank Dr. Uwe Linne (Philipps-University Marburg, Mass Spectrometry Facility) for support during mass spectrometric analyses.

ABBREVIATIONS

3HAA, 3-hydroxyanthranilic acid; 3HK, 3-hydroxykynurenine; 3H4MAA, 3-hydroxy-4-methylanthranilic acid; 3H4MK, 3-hydroxy-4-methylkynurenine; 3,5DH4MAA, 3,5-dihydroxy-4-methylanthranilic acid; 5HAA, 5-hydroxyanthranilic acid; AA, anthranilic acid; DOPA, 3,4-dihydroxyphenylalanine; FAD, flavin adenine dinucleotide; NAD^+ and NADH, nicotinamide adenine dinucleotide; $NADP^+$ and NADPH, nicotinamide adenine dinucleotide phosphate; NRPS, nonribosomal peptide synthetase; PBD, pyrrolo[1,4]benzodiazepine; PLP, pyridoxyl 5′-phosphate; PCP, peptidyl carrier protein; SAM, *S*-adenosylmethionine.

REFERENCES

(1) Parker, K. A., and Babine, R. E. (1982) Revision of assignment of structure to the pyrrolodiazepinone anti-tumor antibiotic sibiromycin. *J. Am. Chem. Soc. 104*, 7330–7331.

(2) Antonow, D., and Thurston, D. E. (2011) Synthesis of DNA-Interactive Pyrrolo[2,1-c][1,4]benzodiazepines (PBDs). *Chem. Rev. 111*, 2815–2864.

(3) Petrusek, R. L., Anderson, G. L., Garner, T. F., Fannin, Q. L., Kaplan, D. J., Zimmer, S. G., and Hurley, L. H. (1981) Pyrrol-[1,4]benzodiazepine antibiotics. Proposed structures and characteristics of the in vitro deoxyribonucleic acid adducts of anthramycin, tomaymycin, sibiromycin, and neothramycins A and B. *Biochemistry 20*, 1111–1119.

(4) Kumar, R., and Lown, J. W. (2003) Recent developments in novel pyrrolo[2,1-c][1,4]benzodiazepine conjugates: Synthesis and biological evaluation. *Mini Rev. Med. Chem. 3*, 323–339.

(5) Kopka, M. L., Goodsell, D. S., Baikalov, I., Grzeskowiak, K., Cascio, D., and Dickerson, R. E. (1994) Crystal structure of a covalent DNA-drug adduct: Anthramycin bound to C-C-A-A-C-G-T-T-G-G and a molecular explanation of specificity. *Biochemistry 33*, 13593–13610.

(6) Clingen, P. H., De Silva, I. U., McHugh, P. J., Ghadessy, F. J., Tilby, M. J., Thurston, D. E., and Hartley, J. A. (2005) The XPF-ERCC1 endonuclease and homologous recombination contribute to the repair of minor groove DNA interstrand crosslinks in mammalian cells produced by the pyrrolo[2,1-c][1,4]benzodiazepine dimer SJG-136. *Nucleic Acids Res. 33*, 3283–3291.

(7) Thurston, D. E., Bose, D. S., Howard, P. W., Jenkins, T. C., Leoni, A., Baraldi, P. G., Guiotto, A., Cacciari, B., Kelland, L. R., Foloppe, M. P., and Rault, S. (1999) Effect of A-ring modifications on the DNA-binding behavior and cytotoxicity of pyrrolo[2,1-c][1,4]benzodiazepines. *J. Med. Chem. 42*, 1951–1964.

(8) Hurley, L. H., and Thurston, D. E. (1984) Pyrrolo-(1,4)Benzodiazepine Antitumor Antibiotics: Chemistry, Interaction with DNA, and Biological Implications. *Pharm. Res. 1*, 52–59.

(9) Gause, G. F., and Dudnik, Y. V. (1971) Interaction of antitumor antibiotics with DNA: Studies on sibiromycin. *Prog. Mol. Subcell. Biol.*, 33–39.

(10) Cargill, C., Bachmann, E., and Zbinden, G. (1974) Effects of daunomycin and anthramycin on electrocardiogram and mitochondrial metabolism of the rat heart. *J. Natl. Cancer Inst. 53*, 481–486.

(11) Lubawy, W. C., Dallam, R. A., and Hurley, L. H. (1980) Protection against anthramycin-induced toxicity in mice by coenzyme Q10. *J. Natl. Cancer Inst. 64*, 105–109.

(12) Kamal, A., Rao, M. V., Laxman, N., Ramesh, G., and Reddy, G. S. (2002) Recent developments in the design, synthesis and structure-activity relationship studies of pyrrolo[2,1-c][1,4]benzodiazepines as DNA-interactive antitumour antibiotics. *Curr. Med. Chem.: Anti-Cancer Agents 2*, 215–254.

(13) Itoh, J., Watabe, H., Ishii, S., Gomi, S., Nagasawa, M., Yamamoto, H., Shomura, T., Sezaki, M., and Kondo, S. (1988) Sibanomicin, a new pyrrolo[1,4]benzodiazepine antitumor antibiotic produced by a *Micromonospora* sp. *J. Antibiot. 41*, 1281–1284.

(14) Antonow, D., Cooper, N., Howard, P. W., and Thurston, D. E. (2007) Parallel synthesis of a novel C2-aryl pyrrolo[2,1-c]-[1,4]benzodiazepine (PBD) library. *J. Comb. Chem. 9*, 437–445.

(15) Tiberghien, A. C., Hagan, D., Howard, P. W., and Thurston, D. E. (2004) Application of the Stille coupling reaction to the synthesis of C2-substituted endo-exo unsaturated pyrrolo[2,1-c][1,4]benzodiazepines (PBDs). *Bioorg. Med. Chem. Lett. 14*, 5041–5044.

(16) Gregson, S. J., Howard, P. W., Hartley, J. A., Brooks, N. A., Adams, L. J., Jenkins, T. C., Kelland, L. R., and Thurston, D. E. (2001) Design, synthesis, and evaluation of a novel pyrrolobenzodiazepine DNA-interactive agent with highly efficient cross-linking ability and potent cytotoxicity. *J. Med. Chem. 44*, 737–748.

(17) Parker, K. A., and Fedynyshyn, T. H. (1979) Synthesis of Anhydrosibiromycinone: New Method for the Direct Synthesis of Pyrrolo-1,4-Benzodiazepin-5-Ones. *Tetrahedron Lett.*, 1657–1660.

(18) Hurley, L. H., and Speedie, M. K., Eds. (1981) *Pyrrolo-(1,4)benzodiazepines antibiotics: Anthramycin, tomaymycin and sibiromycin*, Vol. 4, Springer, Berlin.

(19) Hurley, L. H. (1980) Elucidation and Formulation of Novel Biosynthetic Pathways Leading to the Pyrrolo[1,4]Benzodiazepine Antibiotics Anthramycin, Tomaymycin, and Sibiromycin. *Acc. Chem. Res. 13*, 263–269.

(20) Rokem, J. S., and Hurley, L. H. (1981) Sensitivity and Permeability of the Anthramycin Producing Organism Streptomyces-Refuineus to Anthramycin and Structurally Related Antibiotics. *J. Antibiot. 34*, 1171–1174.

(21) Hu, Y., Phelan, V., Ntai, I., Farnet, C. M., Zazopoulos, E., and Bachmann, B. O. (2007) Benzodiazepine biosynthesis in *Streptomyces refuineus*. *Chem. Biol. 14*, 691–701.

(22) Li, W., Chou, S., Khullar, A., and Gerratana, B. (2009) Cloning and characterization of the biosynthetic gene cluster for tomaymycin, an SJG-136 monomeric analog. *Appl. Environ. Microbiol. 75*, 2958–2963.

(23) Li, W., Khullar, A., Chou, S., Sacramo, A., and Gerratana, B. (2009) Biosynthesis of sibiromycin, a potent antitumor antibiotic. *Appl. Environ. Microbiol. 75*, 2869–2878.

(24) Brahme, N. M., Gonzalez, J. E., Mizsak, S., Rolls, J. R., Hessler, E. J., and Hurley, L. H. (1984) Biosynthesis of the Lincomycins. 2. Studies Using Stable Isotopes on the Biosynthesis of Methylthiolincosaminide Moiety of Lincomycin-A. *J. Am. Chem. Soc. 106*, 7878–7883.

(25) Brahme, N. M., Gonzalez, J. E., Rolls, J. P., Hessler, E. J., Mizsak, S., and Hurley, L. H. (1984) Biosynthesis of the Lincomycins. 1. Studies Using Stable Isotopes on the Biosynthesis of the Propyl-L-Hygric and Ethyl-L-Hygric Acid Moieties of Lincomycin-A and Lincomycin-B. *J. Am. Chem. Soc. 106*, 7873–7878.

(26) Gerratana, B. (2010) Biosynthesis, synthesis, and biological activities of pyrrolobenzodiazepines. *Med. Res. Rev.*.

(27) Golub, E. E., Ward, M. A., and Nishimura, J. S. (1969) Biosynthesis of the actinomycin chromophore: Incorporation of

3-hydroxy-4-methylanthranilic acid into actinomycins by *Streptomyces antibioticus*. *J. Bacteriol. 100*, 977–984.

(28) Gaertner, F. H., and Shetty, A. S. (1977) Kynureninase-type enzymes and the evolution of the aerobic tryptophan-to-nicotinamide adenine dinucleotide pathway. *Biochim. Biophys. Acta 482*, 453–460.

(29) Lima, W. C., Varani, A. M., and Menck, C. F. (2009) NAD biosynthesis evolution in bacteria: Lateral gene transfer of kynurenine pathway in Xanthomonadales and Flavobacteriales. *Mol. Biol. Evol. 26*, 399–406.

(30) Fawaz, F., and Jones, G. H. (1988) Actinomycin synthesis in *Streptomyces antibioticus*. Purification and properties of a 3-hydroxyanthranilate 4-methyltransferase. *J. Biol. Chem. 263*, 4602–4606.

(31) Jones, G. H. (1987) Actinomycin synthesis in *Streptomyces antibioticus*: Enzymatic conversion of 3-hydroxyanthranilic acid to 4-methyl-3-hydroxyanthranilic acid. *J. Bacteriol. 169*, 5575–5578.

(32) Brockmann, H., and Muxfeldt, H. (1958) Actinomycine XIX: Antibiotica aus Actinomyceten XL: Konstitution und Synthese des Actinomycin-Chromophors. *Chem. Ber.*, 1242–1265.

(33) Coric, I., Milic, D., Matkovic-Calogovic, D., and Tomaskovic, L. (2009) Synthesis and crystal structures of two isomeric nitro-α-resorcylic acids. *Struct. Chem.*, 73–80.

(34) Mofid, M. R., Marahiel, M. A., Ficner, R., and Reuter, K. (1999) Crystallization and preliminary crystallographic studies of Sfp: A phosphopantetheinyl transferase of modular peptide synthetases. *Acta Crystallogr. D55*, 1098–1100.

(35) Lambalot, R. H., Gehring, A. M., Flugel, R. S., Zuber, P., LaCelle, M., Marahiel, M. A., Reid, R., Khosla, C., and Walsh, C. T. (1996) A new enzyme superfamily: The phosphopantetheinyl transferases. *Chem. Biol. 3*, 923–936.

(36) Crnovcic, I., Sussmuth, R., and Keller, U. (2010) Aromatic C-methyltransferases with antipodal stereoselectivity for structurally diverse phenolic amino acids catalyze the methylation step in the biosynthesis of the actinomycin chromophore. *Biochemistry 49*, 9698–9705.

(37) Keller, U., Lang, M., Crnovcic, I., Pfennig, F., and Schauwecker, F. (2010) The actinomycin biosynthetic gene cluster of *Streptomyces chrysomallus*: A genetic hall of mirrors for synthesis of a molecule with mirror symmetry. *J. Bacteriol. 192*, 2583–2595.

(38) Pacholec, M., Tao, J., and Walsh, C. T. (2005) CouO and NovO: C-Methyltransferases for tailoring the aminocoumarin scaffold in coumermycin and novobiocin antibiotic biosynthesis. *Biochemistry 44*, 14969–14976.

(39) Lima, S., Kumar, S., Gawandi, V., Momany, C., and Phillips, R. S. (2009) Crystal structure of the *Homo sapiens* kynureninase-3-hydroxyhippuric acid inhibitor complex: Insights into the molecular basis of kynureninase substrate specificity. *J. Med. Chem. 52*, 389–396.

(40) Dua, R., and Phillips, R. S. (1991) Stereochemistry and mechanism of aldol reactions catalyzed by kynureninase. *J. Am. Chem. Soc. 113*, 7385–7388.

(41) Palleroni, N. J., and Stanier, R. Y. (1964) Regulatory Mechanisms Governing Synthesis of the Enzymes for Tryptophan Oxidation by Pseudomonas Fluorescens. *J. Gen. Microbiol. 35*, 319–334.

(42) Shetty, A. S., and Gaertner, F. H. (1973) Distinct kynureninase and hydroxykynureninase activities in microorganisms: Occurrence and properties of a single physiologically discrete enzyme in yeast. *J. Bacteriol. 113*, 1127–1133.

(43) Tanizawa, K., and Soda, K. (1979) Purification and properties of pig liver kynureninase. *J. Biochem. 85*, 901–906.

(44) Walsh, H. A., and Botting, N. P. (2002) Purification and biochemical characterization of some of the properties of recombinant human kynureninase. *Eur. J. Biochem. 269*, 2069–2074.

(45) Moriguchi, M., Yamamoto, T., and Soda, K. (1973) Properties of crystalline kynureninase from *Pseudomonas marginalis*. *Biochemistry 12*, 2969–2974.

(46) Strieker, M., Tanovic, A., and Marahiel, M. A. (2010) Nonribosomal peptide synthetases: Structures and dynamics. *Curr. Opin. Struct. Biol. 20*, 234–240.

(47) Fischbach, M. A., and Walsh, C. T. (2006) Assembly-line enzymology for polyketide and nonribosomal peptide antibiotics: Logic, machinery, and mechanisms. *Chem. Rev. 106*, 3468–3496.

(48) Walsh, C. T., Chen, H., Keating, T. A., Hubbard, B. K., Losey, H. C., Luo, L., Marshall, C. G., Miller, D. A., and Patel, H. M. (2001) Tailoring enzymes that modify nonribosomal peptides during and after chain elongation on NRPS assembly lines. *Curr. Opin. Chem. Biol. 5*, 525–534.

(49) Hubbard, B. K., and Walsh, C. T. (2003) Vancomycin assembly: Nature's way. *Angew. Chem., Int. Ed. 42*, 730–765.

(50) Chen, H., and Walsh, C. T. (2001) Coumarin formation in novobiocin biosynthesis: β-Hydroxylation of the aminoacyl enzyme tyrosyl-S-NovH by a cytochrome P450 NovI. *Chem. Biol. 8*, 301–312.

(51) Rausch, C., Weber, T., Kohlbacher, O., Wohlleben, W., and Huson, D. H. (2005) Specificity prediction of adenylation domains in nonribosomal peptide synthetases (NRPS) using transductive support vector machines (TSVMs). *Nucleic Acids Res. 33*, 5799–5808.

(52) Conti, E., Stachelhaus, T., Marahiel, M. A., and Brick, P. (1997) Structural basis for the activation of phenylalanine in the non-ribosomal biosynthesis of gramicidin S. *EMBO J. 16*, 4174–4183.

(53) Stachelhaus, T., Mootz, H. D., and Marahiel, M. A. (1999) The specificity-conferring code of adenylation domains in nonribosomal peptide synthetases. *Chem. Biol. 6*, 493–505.

(54) Challis, G. L., Ravel, J., and Townsend, C. A. (2000) Predictive, structure-based model of amino acid recognition by nonribosomal peptide synthetase adenylation domains. *Chem. Biol. 7*, 211–224.

(55) Keller, U., Kleinkauf, H., and Zocher, R. (1984) 4-Methyl-3-hydroxyanthranilic acid activating enzyme from actinomycin-producing *Streptomyces chrysomallus*. *Biochemistry 23*, 1479–1484.

(56) Phelan, V. V., Du, Y., McLean, J. A., and Bachmann, B. O. (2009) Adenylation enzyme characterization using γ-$^{18}O_4$-ATP pyrophosphate exchange. *Chem. Biol. 16*, 473–478.

(57) Ishiyama, D., Vujaklija, D., and Davies, J. (2004) Novel pathway of salicylate degradation by *Streptomyces* sp. strain WA46. *Appl. Environ. Microbiol. 70*, 1297–1306.

(58) Strieker, M., Nolan, E. M., Walsh, C. T., and Marahiel, M. A. (2009) Stereospecific synthesis of threo- and erythro-β-hydroxyglutamic acid during kutzneride biosynthesis. *J. Am. Chem. Soc. 131*, 13523–13530.

(59) Helmetag, V., Samel, S. A., Thomas, M. G., Marahiel, M. A., and Essen, L. O. (2009) Structural basis for the erythro-stereospecificity of the L-arginine oxygenase VioC in viomycin biosynthesis. *FEBS J. 276*, 3669–3682.

(60) Ding, W., Deng, W., Tang, M., Zhang, Q., Tang, G., Bi, Y., and Liu, W. (2010) Biosynthesis of 3-methoxy-5-methyl naphthoic acid and its incorporation into the antitumor antibiotic azinomycin B. *Mol. BioSyst. 6*, 1071–1081.

(61) Strieker, M., Essen, L. O., Walsh, C. T., and Marahiel, M. A. (2008) Non-heme hydroxylase engineering for simple enzymatic synthesis of L-threo-hydroxyaspartic acid. *ChemBioChem 9*, 374–376.